Dalton Transactions

PAPER

View Article Online
View Journal | View Issue

Cite this: *Dalton Trans.*, 2016, **45**, 3558

Selective hydrogenation of levulinic acid to γ-valerolactone using *in situ* generated ruthenium nanoparticles derived from Ru–NHC complexes†

Boon Ying Tay,[a,b] Cun Wang,[a] Pim Huat Phua,[a] Ludger Paul Stubbs*[a] and Han Vinh Huynh*[b]

Received 30th August 2015,
Accepted 11th January 2016

DOI: 10.1039/c5dt03366g

www.rsc.org/dalton

Hydrogenation of levulinic acid (LA) to γ-valerolactone (GVL) was studied by using mono- and bidentate *p*-cymene ruthenium(II) N-heterocyclic carbene (NHC) complexes as catalyst precursors. In water, all complexes were found to be reduced *in situ* to form ruthenium nanoparticles (RuNPs) with a high hydrogenation activity. In organic solvents, complexes with monodentate NHC ligands also formed nanoparticles, while complexes with bidentate ligands gave rise to stable homogeneous catalysts with moderate hydrogenation activities.

Introduction

Fossil fuel has always been the main source of energy since the 18th century. However, due to its depletion and related chemical concerns, there has been a shift towards renewable sources of energy and chemicals. Biomass is a suitable alternative as it is the only renewable source of organic carbon.[1] Levulinic acid (LA), which is a product from the hydrolysis of cellulosic biomass, has been suggested by the National Renewable Energy Laboratory as one of the top 12 building block chemicals.[2] By the hydrogenation of LA, γ-valerolactone (GVL) is obtained, which has been suggested as a sustainable liquid for energy and carbon-based chemicals.[3]

The hydrogenation of LA to GVL (Scheme 1) has already been studied since the 1930s with heterogeneous catalysts.[4] In general, this transformation can be achieved by either using homogeneous[5] and heterogeneous[6] catalysts, and a comprehensive review about this topic has been recently published.[6a] Notably, activated carbon supported ruthenium (Ru/C) generally gave the best yields and selectivities in both gas and liquid phase hydrogenations.[6c] Liu *et al.* used 5.0% Ru/C in methanol to achieve a 92% yield GVL in 160 min.[6d] Ru/C was also found to be the most active and product selective towards GVL in the vapour phase hydrogenation of LA.[6e] In addition, Ru nanoparticles have been reported as catalysts, for example by *in situ* reduction from $[Ru_3(CO)_{12}]$.[6h]

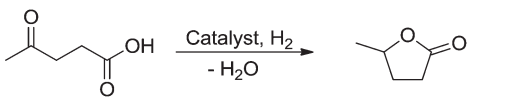

levulinic acid (LA) γ-valerolactone (GVL)

Scheme 1 Conversion of levulinic acid to GVL.

We became interested in the application of N-heterocyclic carbene (NHC) complexes of ruthenium (Ru–NHC) for the hydrogenation of LA. While Ru–NHC complexes have been extensively studied as catalysts for the hydrogenation[7] and transfer hydrogenation[8] of carbonyl compounds, the hydrogenation of LA with Ru–NHC complexes has only recently been explored by Beller *et al.* using catalysts based on $[RuCl_2(p\text{-cymene})]_2$ in dioxane solution with various imidazolium salts as precursors to mono- and bidentate-diNHC ligands.[9] They reported high yields of GVL when bidentate ligands were used, whereas the use of monodentate ligands only resulted in poor yields. To our knowledge, the catalytic activities of well-defined Ru–NHC complexes have not been studied in detail yet.

Herein, we report the synthesis of six *p*-cymene ruthenium(II) mono- and bidentate diNHC complexes and their applications as catalyst precursors in the hydrogenation of LA to GVL. We found that in water, the Ru–NHC complexes were reduced *in situ* by dihydrogen to form ruthenium

[a]*Institute of Chemical and Engineering Sciences, A*STAR (Agency for Science, Technology and Research)., 1 Pesek Road, Jurong Island, 627833 Singapore, Singapore. E-mail: lpstubbs@ices.a-star.edu.sg; Fax: +65 6316 6188; Tel: +65 6796 3813*

[b]*Department of Chemistry, National University of Singapore, 3 Science Drive 3, 117543 Singapore, Singapore. E-mail: chmhhv@nus.edu.sg; Fax: +65 6779 1691; Tel: +65 6516 2670*

†Electronic supplementary information (ESI) available: Experimental details; selected crystallographic data; NMR spectra. CCDC 995422–995424. For ESI and crystallographic data in CIF or other electronic format see DOI: 10.1039/c5dt03366g

nanoparticles (RuNPs) that subsequently catalysed the transformation of LA to GVL with excellent yields in 120–160 min. In organic solvents, complexes with monodentate NHC ligands decomposed to form nanoparticles, while complexes with bidentate ligands formed stable homogeneous catalysts with moderate hydrogenation activities.

Results and discussion

Synthesis of Ru–NHC complexes

The synthetic routes to all ruthenium catalyst precursors are summarised in Scheme 2. The monocarbene ruthenium(II) complexes [$RuCl_2$(*p*-cymene)($^iPr_2$-imy)] (**1**), [$RuCl_2$(*p*-cymene)($^iPr_2$-bimy)] (**2**) and [$RuCl_2$(*p*-cymene)(Bn_2-bimy)] (**3**) derived from imidazole (imy)[10] and benzimidazole (bimy)[11] were prepared as previously reported by deprotonation of the respective azolium salts **A–C** using Ag_2O followed by transmetallation of the resulting silver NHC complexes to [$RuCl_2$(*p*-cymene)]$_2$. The cationic dicarbene complexes [RuCl(η^6-*p*-cymene)(κ^2*C*,*C*-diNHC^{me})][PF_6] (**4**) and [RuCl(η^6-*p*-cymene)(κ^2*C*,*C*-diNHC^{et})][PF_6] (**5**) were similarly obtained by using the diimidazolium dibromides **D** and **E** as ligand precursors instead, followed by anion exchange with KPF_6.[12] A different route to complex **5** and the iodido analogue of **4** by direct deprotonation with triethylamine has been previously reported.[13] Replacement of the diimidazolium salts with the ditopic imidazolium chloride **F** in the latter procedure finally afforded the CN-chelate [RuCl(η^6-*p*-cymene)(κ^2*C*,*N*-NHC-Py)][PF_6] (**6**).[14]

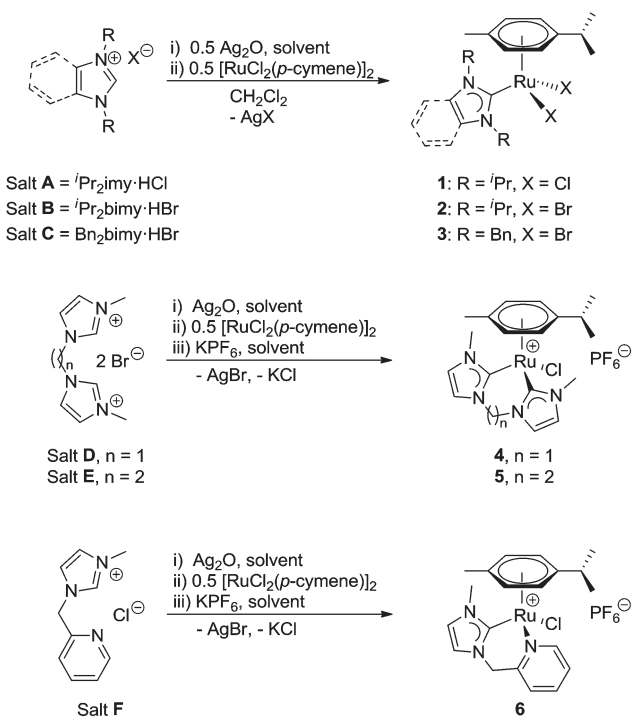

Scheme 2 Syntheses of the *p*-cymene Ru(II) NHC complexes **1–6**.

All six complexes have been isolated as dull yellow to brown solids and were fully characterised by multinuclear NMR spectroscopy, ESI mass spectrometry and elemental analysis providing data, which are generally consistent with the literature reports.

The solid state molecular structures of complexes **2**, **3** and **4** have not been reported, and therefore attempts were made to obtain single crystals suitable for X-ray diffraction. Complexes **2** and **4** could be crystallized by slow diffusion of diethyl ether into a saturated solution in dichloromethane, while crystals of complex **3** formed by slow evaporation of a solution in $CDCl_3$. All complexes show the expected piano–stool structure with the η^6-arene ligand forming the seat, while the carbene, dicarbene and chlorido ligands represent the legs (Fig. 1). This is also observed in complex **1**, which was previously reported.[10] The Ru–centroid distances of neutral complexes **1** to **3** are found to be very similar with values of 1.7066(1) Å,[10] 1.7144(6) Å and 1.6971(4) Å, respectively. The Ru–$C_{carbene}$ distances are identical within 3σ in complexes **1** {2.083(1) Å}, **2** {2.090(3) Å} and **3** {2.089(3) Å}.

The structure of **4** resembles those of **5**[13] and **6**,[14] which were previously reported. Compared to the neutral complexes, the Ru–centroid distances of 1.7391(6) Å observed for **4** is notably longer. The reason for the weaker binding of the arene ligand is the expected reduced back-donation from a more Lewis acidic metal centre in the cationic complex.

The bite angle for **4** is ~83° and smaller than that found for **5** (~87°) due to the increase in the size of the metallacycles moving from a 6- to a 7-membered ring.[13] For complex **6**, a bite angle of ~84° was observed,[14] which is similar to **4** as both contain 6-membered metallacycles. The averaged ruthenium–carbene bond length of 2.044 Å in **4** is significantly shorter than those observed for the neutral complexes. The stronger metal–carbene bonds can be explained by a stronger

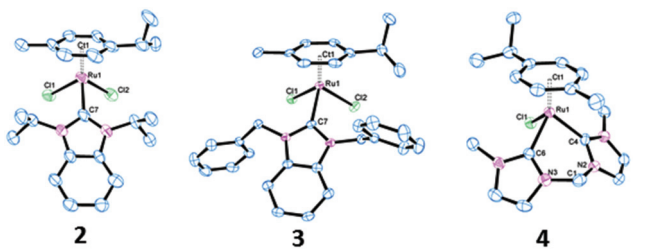

Fig. 1 Molecular structures of **2**, **3** and the cation of **4** with thermal ellipsoids drawn at the 30% probability level. Hydrogen atoms and solvent molecules are omitted for clarity. Selected bond lengths [Å] and bond angles [°] for complex **2**: Ru(1)–C(7) 2.090(3), Ru(1)–Cl(1) 2.4463(12), Ru(1)–Cl(2) 2.4374(11), Ru(1)–Ct1* 1.7144(6); C(7)–Ru(1)–Cl(1) 88.82(8), C(7)–Ru(1)–Cl(2) 89.59(9). Complex **3**: Ru(1)–C(7) 2.089(3), Ru(1)–Cl(1) 2.4068(9), Ru(1)–Cl(2) 2.4267(9), Ru(1)–Ct1* 1.6971(4); C(7)–Ru(1)–Cl(1) 88.96(8), C(7)–Ru(1)–Cl(2) 89.75(8). Complex **4**: Ru(1)–C(4) 2.041(4), Ru(1)–C(6) 2.047(4), Ru(1)–Cl(1) 2.413(1), Ru(1)–Ct1* 1.7391(6); C(4)–Ru(1)–C(6) 83.3(2), N(2)–C(1)–N(3) 109.9(4), C(4)–Ru(1)–Cl(1) 86.3(1), C(6)–Ru(1)–Cl(1) 86.3(1); *Ct1 denotes the centroid of the *p*-cymene ring.

donation from the carbenes to the ruthenium centre in the cationic and thus a more Lewis acidic complex. The ruthenium–chlorido ligands in all complexes are unexceptional and do not require further comments.

Effect of solvents on the hydrogenation of LA to GVL

Complex **1** was chosen as a representative for Ru–NHC complexes for initial catalytic tests. The hydrogenation of LA to GVL using 0.1 mol% of the catalyst precursor at 12 bar dihydrogen pressure and 130 °C for 160 min was studied in various solvents. The results summarised in Table 1 reveal that the highest conversion to GVL was obtained in water (entry 6), while in aprotic organic solvents, significantly lower yields were observed (entries 4 and 5). In methanol, methyl levulinate was the main product (entry 1) with 41% yield. In isopropyl alcohol (IPA), the conversion was very low, with small amounts of GVL and the isopropyl ester formed (entry 3). Under neat conditions, conversion was also insignificant (entry 7).

The activating effect of water on ruthenium catalysts in the hydrogenation of carbonyl compounds is well known, although the reason for it is still disputed. Participation of water in the mechanism has been confirmed by isotope labelling studies.[15,16] Indeed we found that adding water significantly enhances the catalytic activity in methanol and changes the product selectivity to GVL (entry 2). The strong difference in conversion between neat methanol and IPA could possibly be due to residual water traces in methanol.

For all the hydrogenation reactions using catalyst precursor **1**, gradual decolourisation of the initial yellow solution occurred, eventually leaving a black precipitate of ruthenium metal and a colourless supernatant fluid at the end of the reaction (Fig. 2). This observation may indicate the involvement of metal nanoparticles in the catalysis. Indeed, a mercury poisoning test[17] under otherwise identical conditions revealed a large drop of GVL yield from 96% to 31% indicating that the catalysis primarily proceeds in a heterogeneous manner.

The decolourisation and formation of metal precipitate have also been observed by Kühn *et al.* when they used $[Ru(acac)_3]$ without stabilising phosphines as a catalyst in the hydrogenation of LA in water,[6g] and by Sasson *et al.* in their investigation of transfer hydrogenation reactions catalysed by

Table 1 Hydrogenation of LA to GVL in different solvents

Entry	Solvent	Conv. (%)	GVL[a] (%)	TON	TOF (h^{-1})
1	MeOH	45	3 (41)[b]	30	11
2	50% MeOH, 50% water	75	51 (22)	510	191
3	IPA	4	3 (1)[b]	30	11
4	THF	1	1	8	3
5	1,4-Dioxane	2	2	18	7
6	Water	>99	96	963	361
7[c]	Neat	14	5	50	19

Experimental procedure: 4.31 mmol LA, 0.1 mol% **1**, 10 mL solvent, 12 bar H_2, 130 °C, 160 min. [a] Analysis by HPLC. [b] Yield of the corresponding ester in parenthesis. [c] 43.1 mmol LA used (approx. 10 mL).

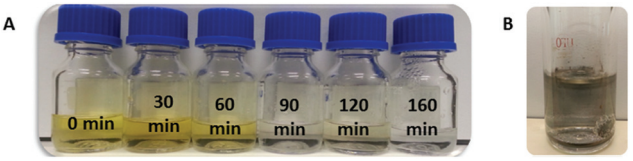

Fig. 2 Appearance of the reaction mixture using complex **1** in water. (A) The reaction mixtures gradually decolourise during the course of hydrogenation from 0 min to 160 min. (B) A colourless supernatant was obtained with metallic coating on the liner wall and magnetic stirrer bar.

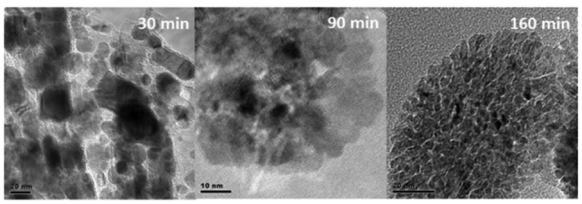

Fig. 3 TEM images of RuNPs formed from **1** in water after 30 min (left), 90 min (middle) and 160 min reaction times (right).

$[RuCl_2(PPh_3)_3]$.[18] Beller *et al.* reported similar low activities for *in situ* formed catalysts from monodentate NHC ligands and $[RuCl_2(p\text{-cymene})]_2$ without giving detailed information about catalyst stability or possible nanoparticle formation.[9] However, they found that bidentate NHC ligands resulted in catalysts with good activities. This intrigued us to test our complexes under similar conditions. Indeed, when using the monodentate NHC complex **2** under their reported reaction conditions (50 bar dihydrogen, 100 °C, dioxane, 6 h) we again found a low yield of 11% GVL, decolourisation and nanoparticle formation (see the ESI† for TEM images). However a yield of 27% GVL, a clear yellow reaction solution and no nanoparticles were found when using bidentate NHC complex **4**. The *In situ* formed catalysts based on diimidazolium salt **D**, $[RuCl_2(p\text{-cymene})]_2$ and KO^{t}Bu also formed stable homogeneous solutions with a similar hydrogenation activity (34% GVL). Obviously, only bidentate NHC ligands can stabilise ruthenium complexes under hydrogenation conditions in non-aqueous solvents.

To gain more insights into the nature of the nanoparticles formed in water, TEM analyses were conducted for the aqueous reaction mixtures of complex **1** after 30, 90 and 160 min (Fig. 3) and also for reaction mixtures with complex **1** in different solvents at 160 min (Fig. 4). It was found that ruthenium nanoparticles (RuNPs) were already formed after 30 min of the reaction in water. The same observation was made for $[RuCl_2(p\text{-cymene})]_2$ and complexes **2–6** (see the ESI†). The nanoparticles were in general found to be clustered. The particle sizes and distributions were similar in all cases, with average particle diameters around 4 nm.

Screening of various pre-catalysts

The activities for the hydrogenation of LA in water obtained with the Ru–NHC catalyst precursors **1–6** were subsequently

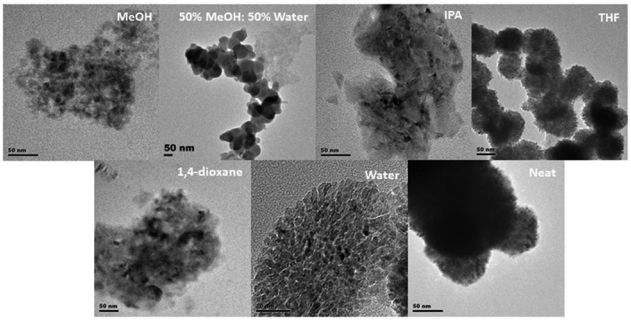

Fig. 4 TEM images of RuNPs formed after 160 min from **1** when different solvents were used for the hydrogenation of LA.

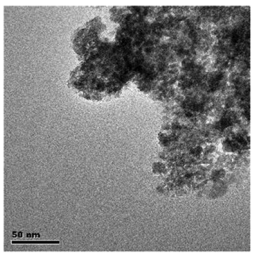

Fig. 5 TEM image of the RuNPs of **1** after one cycle showing significant aggregation.

compared to those of other common ruthenium(II) compounds, and the results are summarised in Table 2. The experimental results were generally reproducible within 2.5% error for the duplicates. Notably, no 1,4-pentanediol as an over-hydrogenated product was found in all cases, even at longer reaction times of 3 hours.

Both Ru/C and $[RuCl_2(p\text{-cymene})]_2$ converted LA to GVL in high TONs of 952 and 995, respectively (entries 1 and 3). The Ru–phosphine complex $[RuCl_2(PPh_3)_3]$, on the other hand, showed a very low activity with a TON of only 137 (entry 3), which is probably due to its low solubility in water.[6g] The monodentate NHC complexes generally gave rise to good hydrogenation catalysts (entries 4–6). The best conversion was found with 1,3-diisopropylbenzimidazolin-2-ylidene complex **2**, where hydrogenation was completed within 120 min (entry 5). Complex **3** with *N*-benzyl wing tip groups led to a markedly lower activity (entry 6). Among the pre-catalysts with bidentate and hetero-bidentate NHC ligands, complex **4** is conspicuously more active than complexes **5** and **6**. In all cases, RuNPs were responsible for the catalytic activity. While the reason for the difference in activities with the different precursors is not clear, it could be speculated that the ligand and complex structure affects the rate of nanoparticle formation or the nanoparticle properties.

In a recycling experiment using complex **1**, another equivalent of LA was added after 160 minutes and 96% conversion to the reaction mixture. The subsequent incremental conversion after 320 min was only 13% (Table 2, entry 10). The TEM images of the reaction mixture showed significant aggregation of the RuNPs (Fig. 5). It occurs that the substrate LA is required to form catalytically active nanoparticles and stabilise them during the course of the reaction. Supporting evidence for this assumption is that RuNPs formed by reduction with dihydrogen in the absence of LA were found to be catalytically inactive.

Kinetic studies

The reaction profiles of $[RuCl_2(p\text{-cymene})]_2$ as well as for complexes **1** to **6** were carried out from 0–160 min with 0.1 mol% pre-catalyst and 12 bar H_2 at 130 °C. For each complex, a series of reactions were performed at different time intervals. This would minimise unpredictable errors from the pressure decrease and the composition differences due to each sampling from a single reaction. The resulting graphs are shown in Fig. 6. The reaction is of zero order in LA concentration for all catalysts (Fig. 6, rate constants in Table 3). Compared with the benchmark catalyst Ru/C, the catalyst derived

Table 2 Hydrogenation of LA to GVL with different pre-catalysts

Entry	Pre-catalyst	GVL (%)[a]	TON	TOF (h^{-1})
1	Ru/C (5%)	95	952	366
2[b]	$[RuCl_2(PPh_3)_3]$	14	137	51
3	$[RuCl_2(p\text{-cymene})]_2$	>99 (63)	995 (629)	373 (315)
4	**1**	96 (68)	963 (683)	361 (342)
5	**2**	>99 (99)	999 (985)	374 (493)
6	**3**	66	660	247
7	**4**	96	961	360
8	**5**	60	595	223
9	**6**	48	480	180
10[c]	**1**	13	120	45

Experimental procedure: 4.31 mmol LA, 0.1 mol% pre-catalyst, 10 mL water, 12 bar H_2, 130 °C, 160 min. [a] Analysis by HPLC, average of 2 runs. [b] Solubility problem in water (yield of GVL at 120 min in parenthesis). [c] Incremental conversion for another 4.31 mmol LA added after 160 minutes under the conditions of entry 4.

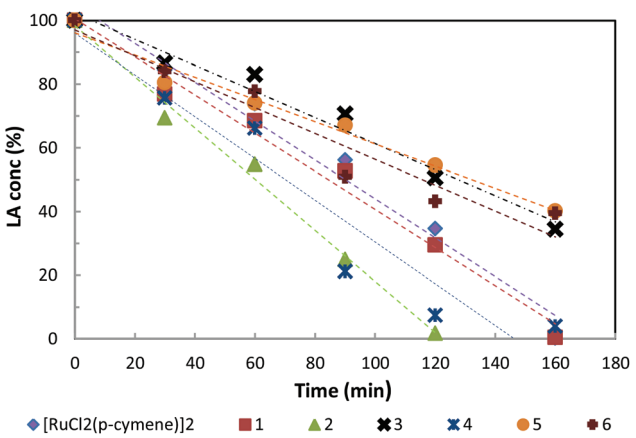

Fig. 6 Plot of LA depletion against time for **1–6** and $[RuCl_2(p\text{-cymene})]_2$.

Table 3 Hydrogenation of LA to GVL with different pre-catalysts

Entry	Pre-catalyst	Rate const. k (M s^{-1})
1	$[RuCl_2(p\text{-cymene})]_2$	4.07×10^{-5}
2	**1**	4.47×10^{-5}
3	**2**	5.90×10^{-5}
4	**3**	2.80×10^{-5}
5	**4**	4.96×10^{-5}
6	**5**	2.75×10^{-5}
7	**6**	3.11×10^{-5}

Table 4 Rate of reactions under 3–15 bar H_2 for **2**

Entry	H_2 pressure (bar)	Reaction rate r (M s^{-1}) for **2**
1	3	0.17×10^{-5}
2	6	3.06×10^{-5}
3	9	5.39×10^{-5}
4	12	7.33×10^{-5}
5	15	8.72×10^{-5}

Reaction conditions: 4.31 mmol LA, 0.1 mol% **2**, 130 °C, 10 mL water, 30 min.

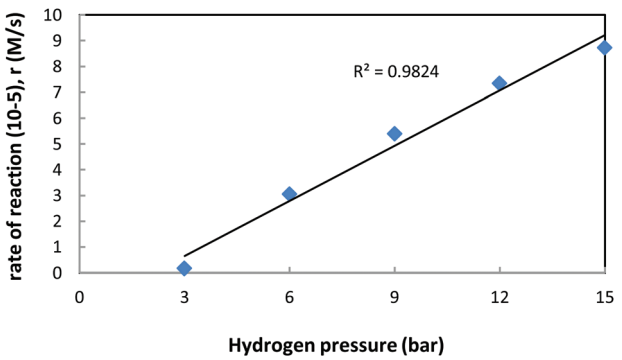

Fig. 7 Hydrogenation of LA to GVL with 0.1 mol% **2** at various pressures (3–15 bar) for 30 min at 130 °C.

from **2** is *ca.* 30% higher in the conversion rate and thus very active. However, catalyst degradation after full conversion (see the previous section) limits the practical applicability.

The effect of hydrogen pressure on reaction rates was studied with catalyst precursor **2** at hydrogen pressures between 3 and 15 bar (Table 4). The reaction is of apparent first order in hydrogen pressure within this range (Fig. 7).

Conclusions

In conclusion, we have prepared a series of mono- and bidentate NHC coordinated ruthenium complexes and demonstrated that they are precursors to active catalysts for the hydrogenation of levulinic acid (LA) to γ-valerolactone (GVL). We found that catalytically active ruthenium nanoparticles are formed from all Ru–NHC complexes under a H_2 atmosphere in water. In organic solvents, complexes with monodentate NHC ligands decompose to ruthenium nanoparticles with low catalytic activity, whereas complexes with bidentate NHC ligands can form stable homogeneous catalysts with moderate hydrogenation activities. For the ruthenium nanoparticles, the rate of the reaction was found to be independent of the LA concentration, but linearly dependent on the dihydrogen pressure within the range of 3–15 bar. To prevent the aggregation of RuNPs as a deactivation pathway, future studies could address the effect of stabilising agents in an attempt to improve the recyclability.

Acknowledgements

We thank the Science and Technology Research Council of A*STAR (Agency for Science, Technology and Research), Singapore for financial support, Ms. Chia Sze Chen for her assistance in X-ray crystallographic analysis, Mr Heng Teck Huat for his assistance in hydrogenation experiments and Ms. Seo Pei Nee for her guidance in TEM analysis.

Notes and references

1 (*a*) G. W. Huber, S. Iborra and A. Corma, *Chem. Rev.*, 2006, **106**, 4044; (*b*) A. Corma, S. Iborra and A. Velty, *Chem. Rev.*, 2007, **107**, 2411.
2 T. Werpy and G. Peterson, U.S. Department of Energy NERL/TP-510-35523, 2004, pp. 45–48.
3 I. T. Horváth, H. Medhi, V. Fábos, L. Boda and L. T. Mika, *Green Chem.*, 2008, **10**, 238.
4 H. A. Schuette and R. W. Thomas, *J. Am. Chem. Soc.*, 1930, **52**, 3010.
5 Selected references for homogeneous hydrogenation: (*a*) K. Osakada, T. Ikariya and S. Yoshikawa, *J. Organomet. Chem.*, 1982, **231**, 79; (*b*) H. Mehdi, V. Fábos, R. Tuba, A. Bodor, L. T. Mika and I. T. Horváth, *Top. Catal.*, 2008, **48**, 49; (*c*) J. M. Tukacs, D. Király, A. Strádi, G. Novodarszki, Z. Eke, G. Dibó, T. Kégl and L. T. Mika, *Green Chem.*, 2012, **14**, 2057; (*d*) F. M. A. Geilen, B. Engendahl, A. Harwardt, W. Marquardt, J. Klankermayer and W. Leitner, *Angew. Chem., Int. Ed.*, 2010, **49**, 5510; (*e*) L. Deng, J. Li, D.-M. Lai, Y. Fu and Q.-X. Guo, *Angew. Chem., Int. Ed.*, 2009, **48**, 6529; (*f*) W. Li, J.-H. Xie, H. Lin and Q. L. Zhou, *Green Chem.*, 2012, **9**, 2388; (*g*) M. Chalid, A. A. Broekhuis and H. J. Heeres, *J. Mol. Catal. A: Chem.*, 2011, **341**, 14.
6 Selected references for heterogeneous hydrogenation: (*a*) W. Wright and R. Palkovits, *ChemSusChem*, 2012, **5**, 1657; (*b*) R. V. Christian, H. D. Brown, Jr. and R. M. Hixon, *J. Am. Chem. Soc.*, 1947, **69**, 1961; (*c*) H. S. Broadbent, G. C. Campbell, W. J. Bartley and J. H. Johnson, *J. Org. Chem.*, 1959, **24**, 1847; (*d*) Z.-P. Yan, L. Lin and S. Liu, *Energy Fuels*, 2009, **23**, 3853; (*e*) P. P. Upare, J.-M. Lee,

D. W. Hwang, S. B. Halligudi, Y. K. Hwang and J.-S. Chang, *J. Ind. Eng. Chem.*, 2011, **17**, 287; (*f*) M. G. Al-Shaal, W. R. H. Wright and R. Palkovits, *Green Chem.*, 2012, **14**, 1260; (*g*) C. Delhomme, L. Schaper, M. Zhang-Preße, G. Raudaschl-Sieber, D. Weuster-Botz and F. E. Kühn, *J. Organomet. Chem.*, 2013, **724**, 297; (*h*) C. Ortiz-Cervantes and J. J. García, *Inorg. Chim. Acta*, 2013, **397**, 124; (*i*) L. Deng, Y. Zhao, J. Li, Y. Fu, B. Liao and Q.-X. Guo, *ChemSusChem*, 2010, **3**, 1172.

7 W. N. O. Wylie, A. J. Lough and R. H. Morris, *Organometallics*, 2012, **31**, 2137.

8 X.-W. Li, G.-F. Wang, F. Chen, Y.-Z. Li, X.-T. Chen and Z.-L. Xue, *Inorg. Chim. Acta*, 2011, **378**, 280.

9 F. A. Westerhaus, B. Wendt, A. Dumrath, G. Wienhöfer, K. Junge and M. Beller, *ChemSusChem*, 2013, **6**, 1001.

10 Y. Zhang, C. Chen, S. C. Ghosh, Y. Li and S. H. Hong, *Organometallics*, 2010, **29**, 1374.

11 S. P. Shan, X. Xiaoke, B. Gnanaprakasam, T. T. Dang, B. Ramalingam, H. V. Huynh and A. M. Seayad, *RSC Adv.*, 2015, **5**, 4434.

12 The transmetallation reactions with salts **D** and **E** also yielded dinuclear ruthenium complexes, where diNHC acts as a bridging ligand. Similar binuclear Ru–NHC complexes have been reported earlier (see: L. Mercs, A. Neels, H. Stoeckli-Evans and M. Albrecht, *Inorg. Chem.*, 2011, **50**, 8188) and hence will not be discussed in this paper. These were separated from mononuclear complexes **5** and **6** by column chromatography.

13 M. Poyatos, E. Mas-Marzá, M. Sanaú and E. Peris, *Inorg. Chem.*, 2004, **43**, 1793.

14 F. E. Fernández, M. C. Puerta and P. Valerga, *Organometallics*, 2012, **31**, 6868.

15 J. Tan, J. Cui, T. Deng, X. Cui, G. Ding, Y. Zhu and Y. Li, *ChemCatChem*, 2015, **7**, 508–512.

16 (*a*) C. Michel, J. Zaffran, A. M. Ruppert, J. Matras-Michalska, M. Jedrzejczyk, J. Grams and P. Sautet, *Chem. Commun.*, 2014, **50**, 12450; (*b*) C. Michel and P. Gallezot, *ACS Catal.*, 2015, **5**, 4130–4132.

17 G. M. Whitesides, M. Hackett, R. L. Brainard, J. P. P. M. Lavalleye, A. F. Sowinski, A. N. Izumi, S. S. Moore, D. W. Brown and E. M. Staudt, *Organometallics*, 1985, **4**, 1819.

18 J. Toubiana and Y. Sasson, *Catal. Sci. Technol.*, 2012, **2**, 1644.